# Asian Journal of Applied Sciences



ISSN 1996-3343

DOI: 10.3923/ajaps.2016.170.177



### **Research Article**

## **Image Analysis for Particle Size Recognition of Bioprocesses in Liquid Environment**

Mayar Aly Atteya, Mohammed A.M. Salem, Doaa Hegazy and Mohammed Ismail Roushdy

Faculty of Computer and Information Sciences, Ain Shams University, Cairo, Egypt

#### **Abstract**

**Background:** Actually, particle size recognition plays an important issue in many applications those applied on microscopic imaging. Today, many developments yield to replace the oil fish ingredients by microalgae products. Indeed, the microalgae cells lives in liquid environment, the size parameter can differentiate between the biological cells, grain stones and air bubbles. **Materials and Methods:** This study presents a method for improving the automation of particle recognition and counting using a recently developed SOPAT-probe (smart on-line particle analysis technology), a photo optical image acquisition device. This method includes image de-noising, image binarization, image enhancement and watershed segmentation. **Results:** This method approves that the microalgae particles can be identified correctly with accuracy reaches up to 99%. **Conclusion:** The proposed method was used to develop an advanced method for a vision-based system that expected to automatically detect, classify and track the active cells using the recently developed SOPAT-system. The result is showed statistically and graphically by computing the area histogram.

Key words: Watershed segmentation, haar wavelet, morphological operations, objects identification, particle size recognition, multi-thresholding, microscopic imaging, *C. cohnni* microalgae

Received: May 27, 2016 Accepted: July 23, 2016 Published: September 15, 2016

Citation: Mayar Aly Atteya, Mohammed A.M. Salem, Doaa Hegazy and Mohammed Ismail Roushdy, 2016. Image analysis for particle size recognition of bioprocesses in liquid environment. Asian J. Applied Sci., 9: 170-177.

Corresponding Author: Mayar Aly Atteya, Faculty of Computer and Information Sciences, Ain Shams University, Cairo, Egypt

Copyright: © 2016 Mayar Aly Atteya *et al.* This is an open access article distributed under the terms of the creative commons attribution License, which permits unrestricted use, distribution and reproduction in any medium, provided the original author and source are credited.

Competing Interest: The authors have declared that no competing interest exists.

Data Availability: All relevant data are within the paper and its supporting information files.

#### **INTRODUCTION**

Seafood (oily fish) plays an important role in human's health¹. It uses in prevention and protection against heart diseases, cancer, diabetes and depressions² and as nutritional supplements in humans and marine organisms in aquaculture³. Now-a-days, many developments yield to replace the fish oil ingredients with the products of biotechnological processes (e.g., marine heterotrophic microalgae), which are used for the production of  $\omega$ -3 (PUFAs) to large amounts (up to 50% of their own cell dry weight) including 30-70% of DHA¹.

The microalgae *Crypthecodinium cohnii* is a small heterotrophic marine dinoflagellate, identified as a good producer of the (DHA)<sup>4,5</sup>. The *C. cohnii* cells grow in submerged culture under optimal conditions, in the dark at 27 in the standard glass vessel stirred tank bioreactor<sup>6</sup>. Among its life cycle, two forms of *C. cohnii* were observed; motile swimming cells and non-motile (cysts). Both forms can be differentiated by the size<sup>5</sup>. Out of one cyst, 1, 2, 4 or 8 swimming daughter cells can originate inside the encapsulated cyst<sup>4,5</sup> as shown in Fig. 1.

Thus, the main concerning in this study is to determine the cell size (visually) for observing the growth rate of these cells. The *C. cohnii* images obtained by SOPAT-probe are evaluated to determine cell concentration, cell size and other relevant parameters simultaneously by automatic image analysis program.

The effective publications of image analysis for bioprocesses were investigated in wide variety of articles. Animal cells were counted by determined three parameters (size of the high pass filter to enforce the shape detection, threshold value used after the hough transformation and the number of circles examined). The correlation coefficient between both reference and data sets had been equal<sup>7</sup> to 0.99.

The images of *Saccharomyces cerevisiae* were processed to evaluate the cell size distribution<sup>8</sup>. The process was based on two parameters (optical properties of cells and threshold value) to facilitate and enhance the problem of cell recognition. It takes about 15 sec per image with error percentage (<2%).

Similar experiments were carried out on liquid and bubbles drops<sup>9,10</sup>, oil drops<sup>11</sup> or crystal drops<sup>12</sup>. However, the most relevant literature of this study was introduced in Guo *et al.*<sup>13</sup>. It had been provided with a strongly method for segmentation according to microalgae features, which composed of image de-noising using haar wavelet transform,

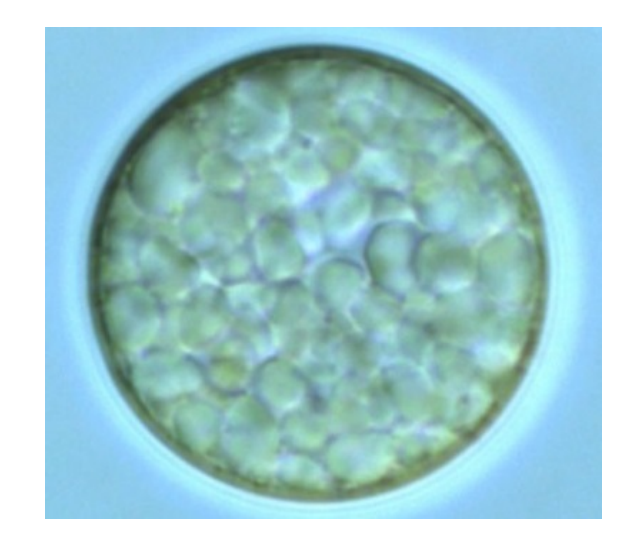


Fig. 1: Cyst with multiple daughter cells inside cell wall. Scale  $bar = 10 \mu m$ 

histogram equalization for quality improving, edge detection and morphological operations to remove debris and gain closed contour for segmented objects.

Actually, this study follows the mentioned approaches taking into consideration the different features of our images and how to process the bottleneck of connected organisms.

#### **MATERIALS AND METHODS**

Based on previous studies, the researchers realize that the image processing and analysis play a major and important role in in-line observation of microorganisms using a microscopic tool.

The proposed method is divided into main five steps; lmage de-noising, image binarization, image enhancement, connected objects separation and cell recognition and localization.

**Wavelet based de-noising processing:** The first step is image de-noising, which is the process of removing the noises out of the captured image. The approach of this process is summarized in three steps: (1) The stationary wavelet transform is applied on the noisy image, (2) The normalization is used to modify the coefficients of wavelet, (3) The inverse discrete stationary wavelet transform are performed to get a de-noising image<sup>3</sup>.

Haar transform is the type of wavelet transform used in the proposed method, it uses scaling and mother wavelet functions<sup>14</sup>. The scaling function represented as:

$$\Phi_{i,k,l}(x, y) = \Phi_{i,k}(x) \Phi_{i,l}(y)$$
 (1)

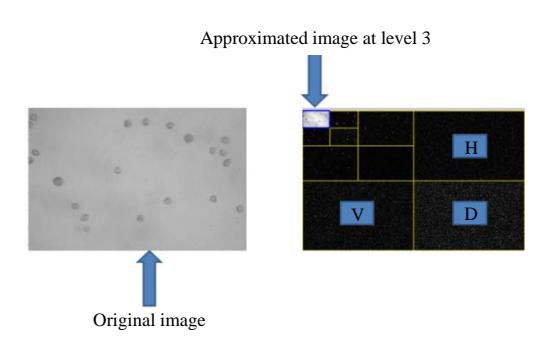


Fig. 2: Two dimensional wavelet analysis, H partition has the horizontal edges, V partition has the vertical edges and D partition has the diagonal edges of the original image

It was described as average function, which used for image approximation. Also, the mother wavelet function was described as the average of difference, which used for image details. It extended into three functions described as:

$$\Psi_{ik,l}^{h}(x,y) = \Phi_{ik}(x)\Psi_{il}(y)$$
 (2)

$$\Psi_{j,k,l}^{v}(x,y) = \Psi_{j,k}(x) \Phi_{j,l}(y)$$
 (3)

$$\Psi_{j,k,l}^{d}(x,y) = \Psi_{j,k}(x)\Psi_{j,l}(y)$$
 (4)

where h, v and d are horizontal, vertical and diagonal details coefficients, respectively (Fig. 2).

Equation 1 was generated by approximating the columns in x-direction and approximating the rows in y-direction. However, the horizontal details obtained by approximating columns in x-direction and detailing rows in y-direction. Vertical details were computed by detail columns in x-direction and approximate rows in y-direction. Since the diagonal image is performed by detail both directions<sup>14,15</sup>.

In order to create a new image that contains the horizontal, vertical and diagonal edges that have been smoothed in the approximation image, the three detailed images are converted to binary images by suitable threshold for each of them. Different threshold algorithms are described by Ruikar and Doye<sup>16</sup> and the penalized threshold method is chosen. It based on sorting the details coefficients in descending order and then computes the threshold value T, as following equation:

$$T = \arg_{t}^{\min} \left[ -\sum_{x=1}^{2} d_{x}^{2} + 2\sigma^{2} t (\alpha + \ln \frac{n}{t}) \right]$$
 (5)

where, t = 1, 2,..., n,  $\alpha$  is sparsity parameter >1 and  $\sigma$  is standard deviation of the zero mean Gaussian white noise in de-noising model<sup>17</sup>.

Finally, the inverse discrete stationary wavelet transform are performed to get a de-noising image<sup>18</sup>.

**Image binarization:** Edge detection is one of the most frequently used techniques in image binarization. An edge is characterized by a high local change of the intensity in image<sup>19</sup>. There are frequently methods used for edge detection. There are: Sobel, canny, roberts, prewitt and log operators. The proposed method uses the mix of sobel and log operators. The following matrix, called sobel kernel. It passes over the image for extracting horizontal and vertical edges<sup>20</sup>:

$$\mathbf{K} = \begin{bmatrix} -1 & 0 & 1 \\ -2 & 0 & 2 \\ -1 & 0 & 1 \end{bmatrix} \tag{6}$$

The log operator used as the method that firstly smoothed the image with Gaussian filter in order to reduce its sensitivity to noise. And then convolve the smoothed image with a laplacian filter. Alternatively, the image was convolved with the linear filter that is the laplacian of Gaussian (LoG kernel):

LoG (x,y) = -1/
$$\pi\sigma^4 [1 - (\frac{x^2 + y^2}{2\sigma^2})]e^{-\frac{x^2 + y^2}{2\sigma^2}}$$
 (7)

The edges can be detected by finding the zero crossing of the 2nd derivative of the image intensity.

Also, image multi-level thresholding has performed on the image as the effective approach of image binarization. Multi-level thresholding determines many threshold values to segment the image into several clusters, C. This is done using a very popular thresholding technique, Otsu's method<sup>21</sup>. It selects an optimal threshold value  $t^*$ , by maximizing  $\sigma_B^2$  as follows:

With:

$$\sigma^{2}B = \sum_{i=1}^{C} \omega_{i} (\mu_{i} - \mu_{T})^{2}$$
 (9)

where,  $\omega_i$  is cumulative of the occurrence probability of grey level and  $\mu_T$  is mean intensity of the whole image.

The proposed method applies the convolution process using sobel kernel, which is favorable for the next operation, image multi-level thresholding. Again the edge detection process is performed using log operator for extracting the strong edges.

**Image enhancement:** In the process of edge detection, based on image quality and original object border gradients, the contour of target would be insufficient. To get closed contour for segmented objects, dilation, erosion, closing and region filling are used on the binary image.

Dilation and erosion are the main morphological operations. Morphological image processing is a collection of non-linear operations related to the shape or morphology of features in an image. Morphological operations rely only on the relative ordering of pixel values, not on their numerical values and therefore are especially suited to the processing of binary images.

Suppose A be an image set and B be a structure element, which main two inputs. The dilation and erosion operations were described as in Eq. 10 and 11, respectively:

$$A \oplus B = (z \in E: B_z \cap A \neq \varphi) \tag{10}$$

$$A \ominus B = (z \in E: B_z \cap A) \tag{11}$$

where, E is euclidean distance =  $Z^2$ ,  $\varphi$  is for the empty set and  $B_z$  is reflection of B;  $B_z = (-b:b \in B)$ .

Simply, closing operation defined as dilation then erosion using the same structuring element for both operations.

The algorithm for region filling is based on set dilations, complementation and intersections as:

$$X_{f} = (X_{f,1} \oplus B) \cap A^{c} \tag{12}$$

where,  $X_0$  is first point inside the boundary,  $A^c$  complement of set<sup>22</sup> A and f = 1, 2, 3.

The results of these operations are influenced by the size and shape of a structuring element B. Actually, the choice of the structuring element must depends on the shape of the objects in the image. Hence, in our case, the adaptive element is the 'Disk-shaped' structuring element based on circular-shaped of the biological objects. According to the objects identification, the dilation process is performed, followed by region filling method to complete the pores of the objects. However, the median filter method for the image is applied to smooth the contour curve after erosion operation.

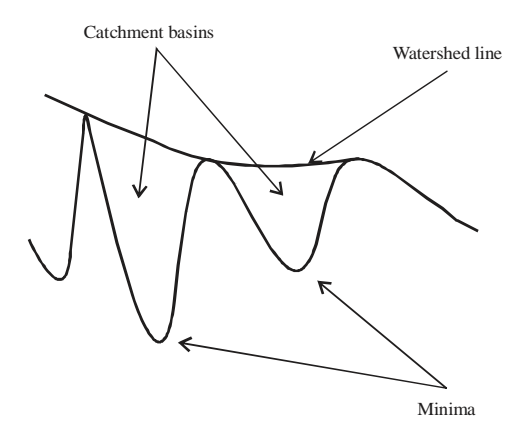


Fig. 3: Topographic surface of grey level image

**Connected objects separation:** It may happen that two or more objects are connected in their borders. Some researchers have neglected these objects. But if the number of connected objects is large with respect to total number of objects, then it causes classification errors<sup>23</sup>. However, the researchers recommend extracting the mutual connected objects using a watershed transformation.

Watershed transformation belongs to region based segmentation. The basic step of this transformation is to visualize a grey image into topographic surface, which includes three notions: minima, catchment basins and watershed lines (Fig. 3).

Each regional minimum of this surface is represented as a catchment basin. The idea of watershed transformation is piercing a hole in each minimum of catchment basin and allowing it to sink in a lake. The water would be inserted gradually from local minimum firstly until fill up different catchment basins of image. When the rising water in different basins were would be to merge, the dams are built to prevent the merging of water coming from two different basins. These boundaries of the dams correspond to the watershed lines which needed to be dividing<sup>24</sup>.

There are various methods of watershed. It can be implemented based on gradient method, marker-controller, distance transform approach, or other algorithms<sup>25,26</sup>. The gradient magnitude method is applied to the gradient images instead of grey level ones<sup>27,28</sup>. This method has an over segmentation problem due to noise in the image. To solve this problem, the marker-controller watershed approach was introduced. It consists of markers to be defined as new minima of the gradient image objects. After segmentation, the watershed line for each object can be separated from its neighbors<sup>25,29</sup>.

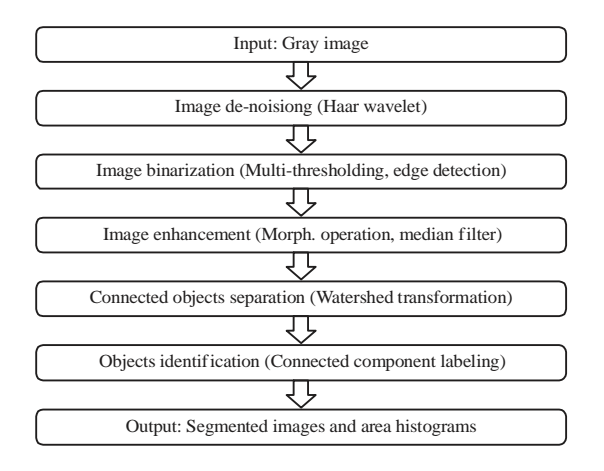


Fig. 4: Proposed approach in a flow diagram

Another approach is the distance transform, which is used in proposed method for segmentation step. It calculates a distance map from the object centre points to the edges of the objects. The centres were determined by performing multiple successive erosions with a suitable structuring element until all foreground regions of the image have been eroded away. Then fills that topological map with imaginary water, where two watersheds meet, it builds a dam to separate them<sup>24,25</sup>. The distance transform provides a metric or measure of the separation of points in the image such as euclidean, city block or chessboard.

The chessboard metric is measuring the path between the pixels based on an 8-connected neighborhood, pixels whose edges or corners touch are one unit apart. The actual structuring element that should be used depends upon which distance metric has been chosen. A  $(3\times3)$  'Square-shaped' element gives the chessboard distance transform.

**Cell characterization:** Cell characterization refers to determine the cell size and other properties. The needing step for this characterization is cell recognition, identification and separation of cell pixels from the surrounding non-cell pixels of the background<sup>8</sup>. The object is recognized by computing connected component labelling operation after applying the previous methodologies of the proposed approach<sup>30</sup>. From this point, the authors can determine the cells number in each input image to measure the concentration of cells during the growth. After that, relevant cell size parameters could be obtained. Area, perimeter, diameter and radius of each cell could be calculated.

Figure 4 is summarizing up the steps of the proposed method presented so far.

#### **RESULTS AND DISCUSSION**

The proposed approach is applied on data set of the real images of *C. cohnii* cells whose growth in liquid environment. The cells are tracked by SOPAT-probe for 1, 18 and 42 h for giving producer cells. Figure 4 and 5 represent the output of each step in the experiment according to the steps mentioned in Fig. 4.

Figure 5a gives the initial grey image. Figure 5b shows the first step in the method, de-noising the image using Haar wavelet technique as a pre-processing step for image binarization. The microalgae microscopic images are processed by the haar wavelet transform. The initial image is decomposed for three levels and the hard thresholds are chosen for all levels. This can not only eliminate noise effectively but also retain edge's information at the most extent. The next step, image convolution by Sobel kernel is shown in Fig. 5c and for more clarification, the image contrast is adjusted as shown in Fig. 5d.

For binary image, the multi-thresholding using Otsu's method is applied, followed by edge detection method via log operator (Fig. 6a). The log parameters assigning as: t=0.0005,  $\sigma=2.5$ . In the resulting image, a clear identification of the cells could not be identified. Hence, the needing to some enhancements is crucial.

Starting the enhancement by close and dilate the objects to identify the features of cells as shown Fig. 6b. Even if the dilation of the cells borders may leads to connect previously unconnected cells, the watershed segmentation will be able to overcome this issue.

However, for getting more identification, filling object's hole is applied Fig. 6c. The resulting image is not optimal one due to the large amount of debris. The authors have to solve this problem by applying one of the morphological operations, erosion, with "Disk-shaped" structure element of size "10". In order to remove such debris and get the circular edges more smoothed, median filter technique is applied with a mask window  $(9 \times 9)$  (Fig. 6d).

Next, the problem of connected objects was faced which are segmented as one component, as shown in Fig. 6. However, the important objective is to find the area size of the individual object. So, the distance transform chessboard along with watershed is used to segment mutually connecting objects and the result shown in Fig. 7.

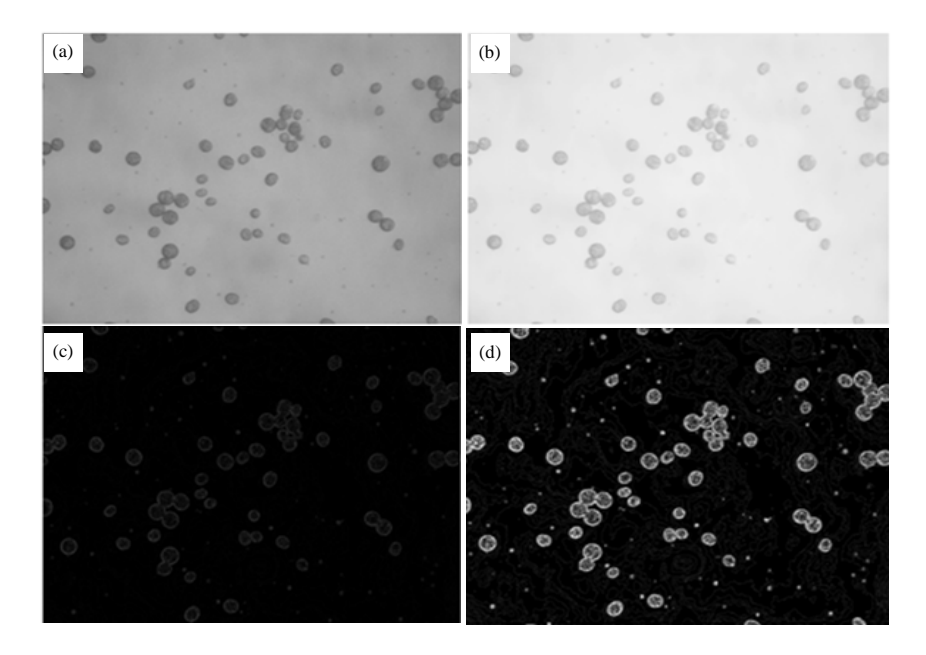


Fig. 5(a-d): (a) Grey scale image of microalgae, (b) De-noised image of microalgae by haar wavelet method, (c) Image convolution using sobel kernel and (d) Image adjustment

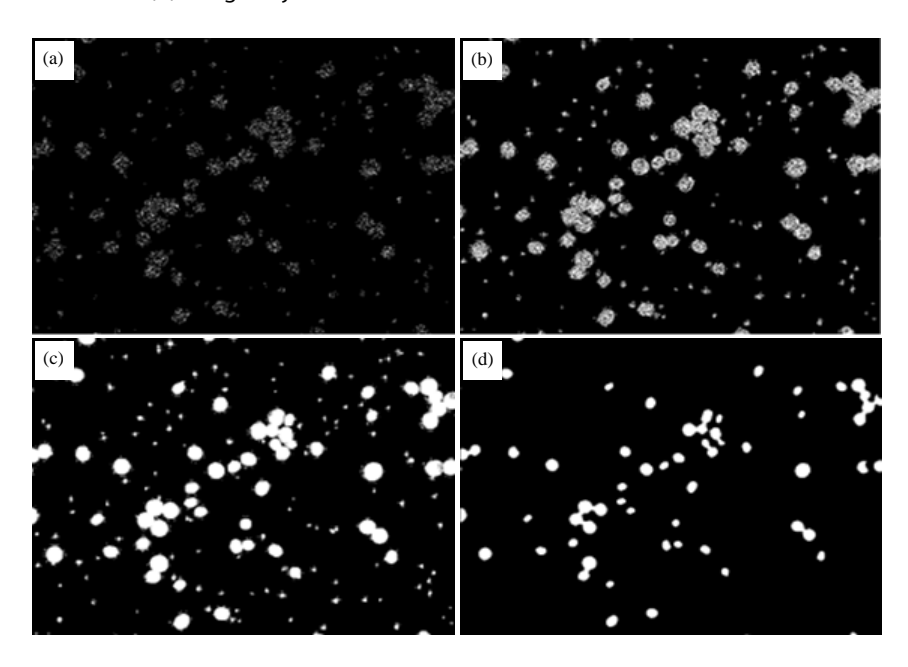


Fig. 6(a-d): (a) Binary image of microalgae, (b) Image after closing and dilation, (c) Image after filling holes and (d) Image after erosion and median filter

Now, the cell's size can be computed for each object separately. By compute an area histogram for the tested images (1, 18 and 42 h), the variation is observed. The cell concentration has been clearly increased which is an evidence for true or correct growth rate. First image has 22 cells and the number of the cells is increased to be 55 in the second image and finally the number increased again to be 66 in the third image. Figure 8 shows the area histogram of the given images.

Actually, the size parameter can differentiate between the cells. In this case, the cells with radius greater than or equal to<sup>29</sup> are classified as active cells. Other radius could identify as air bubbles, grain stone, or motile cells.

The accuracy is given by calculating the average values of this metric for the input images (Table 1). However, the remaining accuracy percentage is missed because the over segmentation resulting from watershed step.

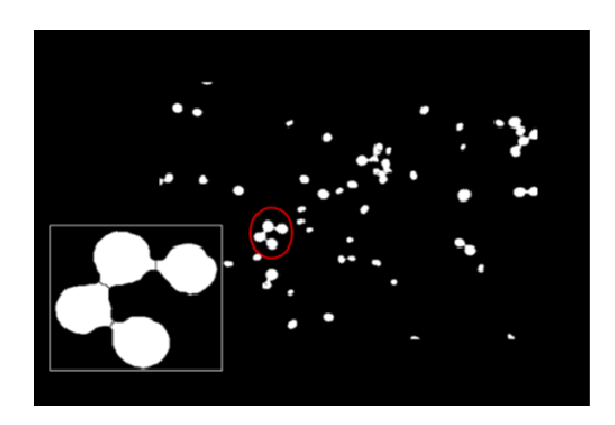
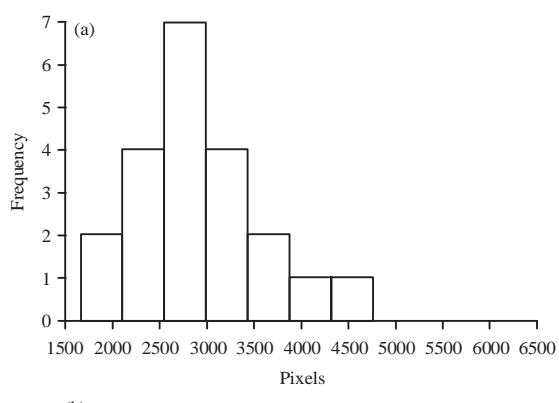
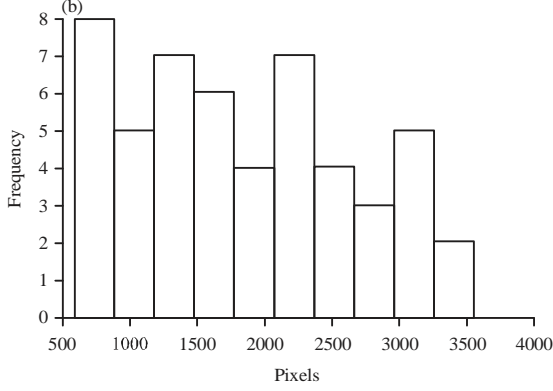


Fig. 7: Image after watershed segmentation





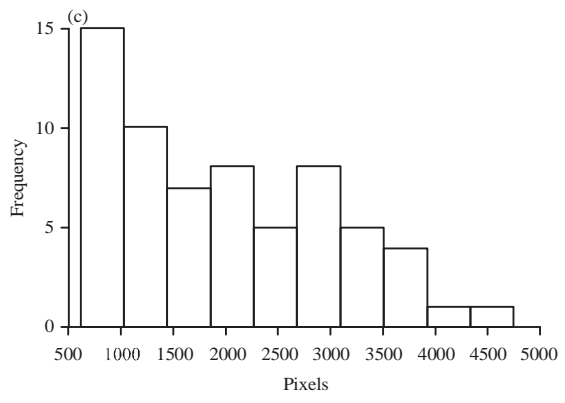


Fig. 8(a-c): Area histogram (in pixels) of bio-cells for 1, 18 and 42 h

Table 1: Accuracy percentage for input images

	1 h (1)	18 h (1)	42 h (1)	1 h (2)	18 h (2)
True objects	22	55	66	58	100
Detected objects	22	54	65	58	99
Percentage (%)	100	98	99	100	99

#### CONCLUSION

In this study, a method for in-line identification of micro-organisms has been presented. The method includes image de-noising using haar wavelets, image convolution by sobel operator, image binarization using multi-thresholding method and edge extraction, image enhancement by such morphological operations, connected objects extraction using watershed method and cell recognition and localization. However, the calculated values correlate very well with those obtained by manually analysis with accuracy reached up to 99%.

#### SIGNIFICANT STATEMENTS

In this study, the researchers concern on the development of a biotechnological process, where an advanced inline imaging technology is strongly needed in order to follow morphologic changes of the microalgae cells. This observation is crucial for the process yield, while cells should be kept in a certain stage. The study should be of interest to readers in the areas of image processing and cell biology.

#### **ACKNOWLEDGMENTS**

Many thanks were provided to Dr. Ing. Stefan Junne and Prof. Dr. Peter Neubauer, chair of Bioprocess Engineering, Berlin University of Technology, for making the data sets available for our study.

#### **REFERENCES**

- Martins, D.A., L. Custodio, L. Barreira, H. Pereira, R. Ben-Hamadou, J. Varela and K.M. Abu-Salah, 2013. Alternative sources of *n*-3 long-chain polyunsaturated fatty acids in marine microalgae. Mar. Drugs, 11: 2259-2281.
- Mendes, A., P. Guerra, V. Madeira, F. Ruano, T.L. da Silva and A. Reis, 2007. Study of docosahexaenoic acid production by the heterotrophic microalga *Crypthecodinium cohnii* CCMP 316 using carob pulp as a promising carbon source. World J. Microbiol. Biotechnol., 23: 1209-1215.
- 3. Perez-Garcia, O., F.M.E. Escalante, L.E. de-Bashan and Y. Bashan, 2011. Heterotrophic cultures of microalgae: Metabolism and potential products. Water Res., 45: 11-36.

- 4. Prabowo, D.A., O. Hiraishi and S. Suda, 2013. Diversity of *Crypthecodinium* spp. (Dinophyceae) from Okinawa prefecture, Japan. J. Mar. Sci. Technol., 21: 181-191.
- De Swaaf, M.E., 2003. Docosahexaenoic Acid Production by the Marine Alga Crypthecodinium Cohnii. IOS Press, USA., ISBN: 9789040724008, Pages: 127.
- Bhaud, Y., J.M. Salmon and M.O. Soyer-Gobillard, 1991. The complex cell cycle of the dinoflagellate protoctist *Crypthecodinium cohnii* as studied *in vivo* and by cytofluorimetry. J. Cell Sci., 100: 675-682.
- Guez, J.S., J.P. Cassar, F. Wartelle, P. Dhulster and H. Suhr, 2004. Real time *in situ* microscopy for animal cell-concentration monitoring during high density culture in bioreactor. J. Biotechnol., 111: 335-343.
- 8. Bittner, C., G. Wehnert and T. Scheper, 1998. *In situ* microscopy for on-line determination of biomass. Biotechnol. Bioeng., 60: 24-35.
- Galindo, E., C.P. Larralde-Corona, T. Brito, M.S. Cordova-Aguilar, B. Taboada, L. Vega-Alvarado and G. Corkidi, 2005. Development of advanced image analysis techniques for the *in situ* characterization of multiphase dispersions occurring in bioreactors. J. Biotechnol., 116: 261-270.
- Bras, L.M.R., E.F. Gomes, M.M.M. Ribeiro and M.M.L. Guimaraes, 2009. Drop distribution determination in a liquid-liquid dispersion by image processing. Int. J. Chem. Eng. 10.1155/2009/746439.
- 11. Dominguez, A.R. and G. Corkidi, 2011. Automated recognition of oil drops in images of multiphase dispersions via gradient direction pattern. Proceedings of the 4th International Congress on Image and Signal Processing, Volume 3, October 15-17, 2011, Shanghai, pp: 1209-1213.
- 12. Presles, B., J. Debayle, A. Rivoire, J.C. Pinoli and G. Fevotte, 2009. *In situ* particle size measurements during crystallization processes using image analysis. Actes de la XII° Congres de la Societe Francaise de Genie des Procedes Pour Relever les Defis Industriels du XXI° Siecle a la Croisee des Sciences et des Cultures, October 14-16, 2009, Marseille, France, pp: 1-6.
- 13. Guo, X., H. Liu and F. Jiang, 2010. Research on the segmentation method of micro algae image. Math. Phys. Fish. Sci., 8: 1-7.
- 14. Ismail, B. and A. Khan, 2012. Image de-noising with a new threshold value using wavelets. J. Data Sci., 10: 259-270.
- 15. Salem, M.A.M., 2011. Medical Image Segmentation: Multiresolution-Based Algorithms. VDM Verlag, Saarbrucken, Germany.
- 16. Ruikar, S.D. and D.D. Doye, 2011. Wavelet based image denoising technique. Int. J. Adv. Comput. Sci. Applic., 2:49-53.

- 17. Moghtased-Azar, K. and M. Gholamnia, 2014. Effect of using different types of threshold schemes (in wavelet space) on noise reduction over GPS times series. J. Geomatics Sci. Technol., 4: 51-66.
- 18. Raviraj, P. and M.Y. Sanavullah, 2007. The modified 2D-Haar wavelet transformation in image compression. Middle-East J. Scient. Res., 2: 73-78.
- 19. Maini, R. and H. Aggarwal, 2009. Study and comparison of various image edge detection techniques. Int. J. Image Process., 3: 1-12.
- Vincent, O.R. and O. Folorunso, 2009. A descriptive algorithm for sobel image edge detection. Proceedings of the Informing Science+IT Education Conference, June 12-15, 2009, Macon State College, Macon, GA., USA., pp: 97-107.
- 21. Huang, D.Y., T.W. Lin and W.C. Hu, 2011. Automatic multilevel thresholding based on two-stage Otsu's method with cluster determination by valley estimation. Int. J. Innovat. Comput. Inform. Control, 7: 5631-5644.
- 22. Raid, A.M., W.M. Khedr, M.A. El-Dosuky and M. Aoud, 2014. Image restoration based on morphological operations. Int. J. Comput. Sci. Eng. Inform. Technol., 4: 9-21.
- 23. Pons, M.N. and H. Vivier, 2000. Biomass quantification by image analysis. Adv. Biochem. Eng./Biotechnol., 66: 133-184.
- 24. Lu, N. and X. Ke, 2007. A segmentation method based on gray-scale morphological filter and watershed algorithm for touching objects image. Proceedings of the 4th International Conference on Fuzzy Systems and Knowledge Discovery, Volume 3, August 24-27, 2007, Haikou, pp: 474-478.
- 25. Kaur, A. and Aayushi, 2014. Image segmentation using watershed transform. Int. J. Soft Comput. Eng., 4: 5-8.
- 26. Beucher, S., 1992. The watershed transformation applied to image segmentation. Scanning Microsc. Int., 6: 299-314.
- 27. Belaid, L.J. and W. Mourou, 2009. Image segmentation: A watershed transformation algorithm. Image Anal. Stereol., 28: 93-102.
- 28. Jackway, P.T., 1996. Gradient watersheds in morphological scale-space. IEEE Trans. Image Proces., 5: 913-921.
- 29. Lopez-Mir, F., V. Naranjo, J. Angulo, E. Villanueva, M. Alcaniz and S. Lopez-Celada, 2011. Aorta segmentation using the watershed algorithm for an augmented reality system in laparoscopic surgery. Proceedings of the 18th IEEE International Conference on Image Processing, September 11-14, 2011, Brussels, pp: 2649-2652.
- Di Stefano, L. and A. Bulgarelli, 1999. A simple and efficient connected components labeling algorithm. Proceedings of the International Conference on Image Analysis and Processing, September 27-29, 1999, Venice, Italy, pp: 322-327.